

# Convective Cooling of Lightning Channels

12

J. M. PICONE AND J. P. BORIS

*Laboratory for Computational Physics*

LEVEL II

J. R. GREIG AND M. RALEIGH

*Experimental Plasma Physics Branch  
Plasma Physics Division*

and

R. F. FERNSLER

*JAYCOR, Inc.  
Alexandria, VA 22304*

DTIC  
ELECTE  
APR 21 1981  
S D E

April 14, 1981

This research was supported by the Office of Naval Research and by the Defense Advanced Research Projects Agency (DoD) ARPA Order No. 3718, monitored by the Naval Surface Weapons Center under Contract N60921-80-WR-W0189.



**NAVAL RESEARCH LABORATORY**  
Washington, D.C.

Approved for public release; distribution unlimited.

81 4 20 074

AD A 097994

UNC FILE COPY

(14) NRL-MR-4472

SECURITY CLASSIFICATION OF THIS PAGE (When Data Entered)

9 REPORT DOCUMENTATION PAGE		READ INSTRUCTIONS BEFORE COMPLETING FORM	
1. REPORT NUMBER NRL Memorandum Report 1472	2. GOVT ACCESSION NO. AD-A097994	3. RECIPIENT'S CATALOG NUMBER	
4. TITLE (and Subtitle) CONVECTIVE COOLING OF LIGHTNING CHANNELS.		5. TYPE OF REPORT & PERIOD COVERED Interim report on a continuing NRL problem.	
6. AUTHOR(s) J. M. Picone, J. P. Boris, J. R. Greig, M. Raleigh and R. F. Fernsler		7. PERFORMING ORG. REPORT NUMBER 15 J. ARPA Order 3718	
8. PERFORMING ORGANIZATION NAME AND ADDRESS Naval Research Laboratory Washington, DC 20375	(12) 29	10. PROGRAM ELEMENT, PROJECT, TASK AREA & WORK UNIT NUMBERS 61153N/RR0330244/44-0756-0-1 and 61101E; 0; OR40AA	(17)
11. CONTROLLING OFFICE NAME AND ADDRESS Office of Naval Research, Arlington, VA 22217 and Defense Advanced Research Projects Agency, Arlington, VA 22209	(11) 14	12. REPORT DATE April 1981	
14. MONITORING AGENCY NAME & ADDRESS (if different from Controlling Office) Naval Surface Weapons Center White Oak, MD 20910	(16) RR03302	13. NUMBER OF PAGES 28	
		15. SECURITY CLASS. (of this report) UNCLASSIFIED	
		15a. DECLASSIFICATION/DOWNGRADING SCHEDULE	
16. DISTRIBUTION STATEMENT (of this Report) Approved for public release; distribution unlimited.			
17. DISTRIBUTION STATEMENT (of the abstract entered in Block 20, if different from Report)			
18. SUPPLEMENTARY NOTES This research was supported by the Office of Naval Research and by the Defense Advanced Research Projects Agency (DoD) ARPA Order No. 3718, monitored by the Naval Surface Weapons Center under Contract N60921-80-WR-W0189. *Present address: JAYCOR, Inc., Alexandria, VA 22304			
19. KEY WORDS (Continue on reverse side if necessary and identify by block number) Lightning Nitrogen fixation Convective cooling Electric discharges			
20. ABSTRACT (Continue on reverse side if necessary and identify by block number) We report experimental data which trace the time development of electric discharge channels in air and which demonstrate the turbulent cooling of such channels. These data provide qualitative confirmation of the model proposed and used by Hill, Rinker, and Wilson to calculate the production of nitrogen oxides by lightning. We outline an analytical treatment which identifies asymmetries in the pressure and density gradients of the discharge channel as a significant source of vorticity. The vorticity, in turn, causes ambient air to mix into the channel. Our theoretical analysis results in (Continues)			

DD FORM 1473 1 JAN 73

EDITION OF 1 NOV 65 IS OBSOLETE  
S/N 0102-014-6601

SECURITY CLASSIFICATION OF THIS PAGE (When Data Entered)

251950

JW

20. ABSTRACT (Continued)

equations from which the vorticity strength and mixing time scale may be calculated. We briefly describe detailed simulations with which we have calibrated the theory. Finally, we combine the experimental data with our calibrated formulas to estimate the convective mixing rate in the case of lightning. We obtain a rate of  $\sim 300 \text{ cm}^3/\text{sec}$  per  $\text{cm}^3$  air in the return stroke channel after pressure equilibrium has been achieved.

about 300 cc/sec/cc

CONTENTS

INTRODUCTION ..... 1

EXPERIMENTAL STUDIES ..... 2

THEORETICAL AND NUMERICAL STUDIES ..... 4

ACKNOWLEDGMENT ..... 14

REFERENCES ..... 15

APPENDIX ..... 17

Accession For	
NTIS GRA&I	<input checked="" type="checkbox"/>
DTIC TAB	<input type="checkbox"/>
Unannounced	<input type="checkbox"/>
Justification	
By _____	
Distribution/	
Availability Codes	
Dist	Avail and/or Special
<b>A</b>	

## CONVECTIVE COOLING OF LIGHTNING CHANNELS

### 1. Introduction

Hill et al. (1980) have recently proposed a "channel heating" model to predict the production of atmospheric nitrogen oxides ( $\text{NO}_x$ ) by lightning. In this model, the return stroke deposits energy over  $\sim 100 \mu\text{s}$ , heating the lightning channel to  $\sim 30000\text{K}$  within a few microseconds. As energy is deposited, the heated region (i.e., the channel) expands and compresses the atmosphere surrounding the channel to produce a shock wave. Subsequently, the shock wave decouples from the channel as the return stroke current drops to small values. The channel continues to expand until pressure equilibrium is reached with the surrounding air at a temperature of  $\sim 3000\text{K}$ . The rate at which the air inside the channel cools is important to the calculation of  $\text{NO}_x$  production by lightning. Hill et al. (1980) calculated the production rate based on the assumption of "turbulent" or convective cooling, in which the ambient air is mixed with the air inside the channel at a prescribed constant rate. The authors used a detailed air chemistry computer code to simulate cooling at several rates, the lower limit of which was based on the rate of cooling by thermal conduction in the absence of convective mixing. They left open questions regarding the cause of the convective cooling, the efficiency of mixing, and the length of the time interval between pressure equilibration of the channel and the onset of mixing.

In this note, we report experimental data which directly confirm qualitative aspects of the above model and which demonstrate the turbulent cooling of discharge channels. We then outline a preliminary analytical treatment which identifies asymmetries in the pressure and density gradients of the discharge channel as a significant source of vorticity, which in turn causes the ambient air to mix into the channel. Our theoretical analysis results

Manuscript submitted January 12, 1981.

in equations from which the vorticity strength and the mixing time scale may be calculated. To calibrate this analytic model and test its predictions, we have performed detailed, two-dimensional numerical simulations which will be described briefly and compared with our analytic results. Finally, we combine the experimental data with our calibrated formulas to estimate the convective mixing rate in the case of lightning.

## 2. Experimental Studies

We have recently performed experimental studies of the propagation of electric discharges through air and the dynamics of the resulting channels (Greig, et al., 1978). In Fig. 1, we show Schlieren photographs of discharges which were 15 cm in length. The discharges were produced by a Marx generator with an erected voltage of  $\sim 250$  kV. The current had a peak value of  $\sim 10$  kA, a period of  $\sim 3\mu\text{s}$ , and a duration of  $\sim 6\mu\text{s}$ . While this is a much shorter pulse than that occurring in a lightning return stroke, we expect the qualitative behavior to be similar after the shock decouples from the channel because air response in rotational flow is relatively slow. We have, in fact, performed preliminary experiments using parameters similar to those of a lightning return stroke. We could not, however, obtain a complete sequence of photographs similar to Fig. 1 because the channel size exceeded the capability of our optical system.

In Fig. 1, we see that a hot, smooth, curved channel with a radius of  $\sim 1.4$  cm has formed within  $8\mu\text{s}$  of the initiation of the discharge. The accompanying shock wave has already decoupled from the channel and appears as a sharp line at the boundary. By  $30\mu\text{s}$ , the shock is easily identifiable and propagates out of the field of view at a time somewhat greater than  $100\mu\text{s}$  after discharge initiation. At approximately  $100\mu\text{s}$ , the interior temperature of the channel is  $\sim 5000\text{K}$ , the gas density is  $\sim 10^{18}\text{cm}^{-3}$  and the electron density is

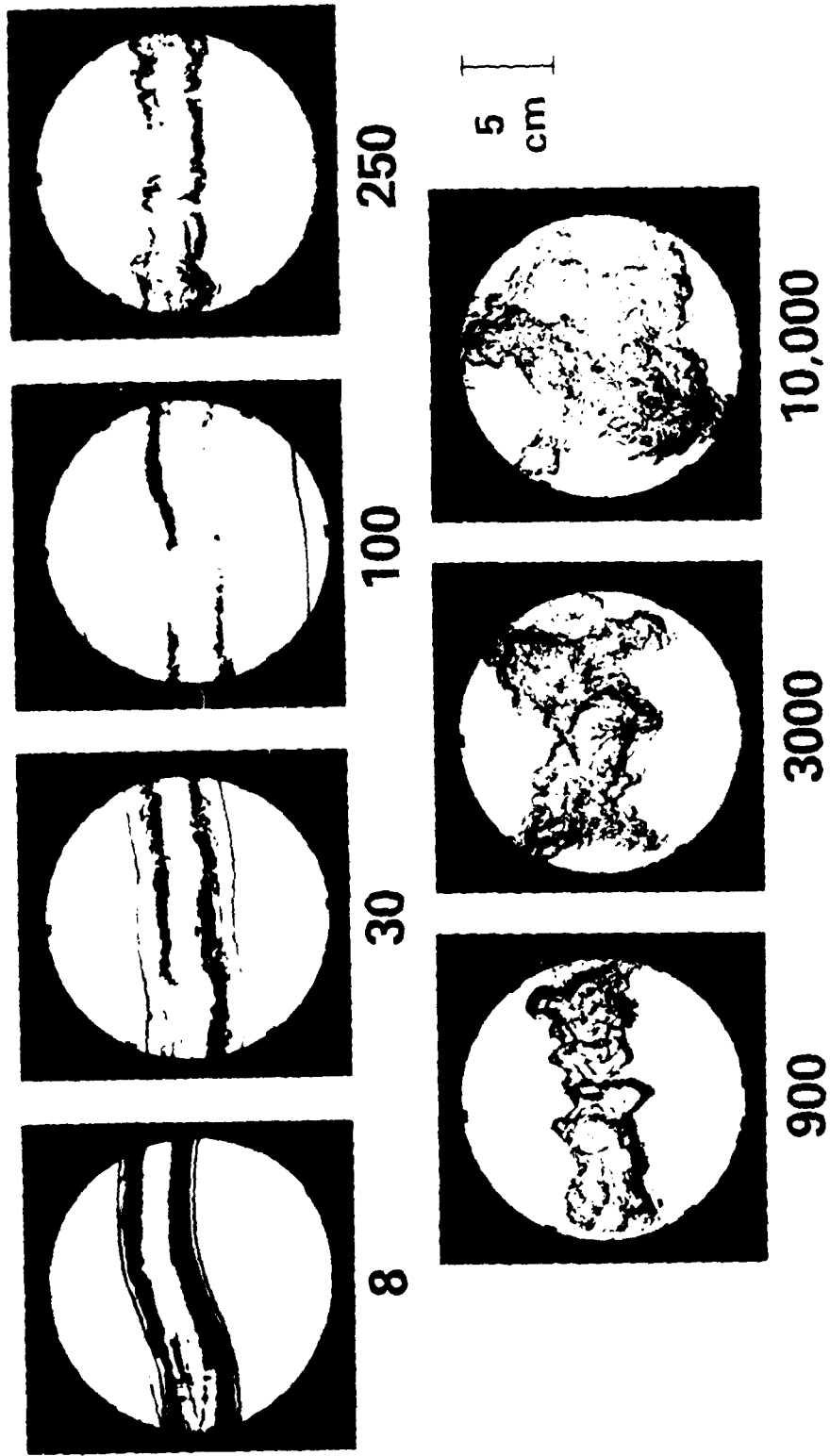


Fig. 1 — Schlieren photographs of unguided discharges in the atmosphere; discharge length 15 cm; voltage ~ 250 kV. The time at which each photograph was taken is given in microseconds; the exposure time was 25 nsec. Note that the photographs depict separate, normally identical discharges.

$\sim 10^{14} \text{ cm}^{-3}$ . (These values are the measured conditions for a comparable discharge in a pre-ionized channel.) The heated channel remains roughly stable up to that point. By 250 $\mu$ s, however, instability has begun to distort the channel, as evidenced by density fluctuations at the channel boundary. The photograph at 900 $\mu$ s shows that the distortions become more pronounced as cooler air at the edges of the channel is pulled toward the axis. The average radius has also increased to  $\sim 2$ cm, indicating an increase of  $\sim 100\%$  in the volume of the channel due to entrainment of the surrounding air. As the time from discharge initiation increases, smaller scale (turbulent) structure appears and by 10ms, the channel has begun to disappear. We estimate the final channel radius to be  $\sim 6-7$ cm, indicating a volume increase of  $\sim 20$  times the original volume. Studies of similar discharges, which have been guided along a path designated by laser/aerosol interaction, have produced nearly identical results. Channel cooling and the onset of turbulence were somewhat more rapid for such "laser-guided discharges." This result follows directly from the analytic theory described in the next section.

### 3. Theoretical and numerical studies

Our theoretical treatment<sup>2</sup> attributes the "turbulent" (convective) cooling phenomenon to asymmetries between the gradients of the existing pressure and density distributions. These asymmetries will generate vorticity as the channel expands, according to the equation

$$\frac{d}{dt} \tilde{\xi} + \tilde{\xi} \cdot \tilde{v} = \tilde{\xi} \cdot \tilde{\nabla} \tilde{v} + (\tilde{\nabla} \rho \times \tilde{\nabla} P) / \rho^2, \quad (1)$$

where

$$\tilde{\xi} = \tilde{\nabla} \times \tilde{v} \quad (2)$$

is the vorticity,  $\tilde{v}$  is the fluid velocity,  $\rho$  is the density, and  $P$  is the pressure. All of the variables are functions of the position  $\tilde{r}$  and the time  $t$ . Following expansion of the channel to achieve pressure equilibrium,

a significant residual vorticity exists. This vorticity is responsible for mixing of ambient air with the hot channel gas. We should point out that other mechanisms for generating residual vorticity in the heated channel might exist. For example, rapid movement of the discharge current axis may occur as a result of magnetic forces present when the current is nonnegligible. Such movement could cause sufficient displacement of the surrounding air to produce some long-term mixing motion. We will reserve consideration of such phenomena for a future, more detailed paper.

We have identified several types of asymmetry which might be relevant to lightning and the above discharge experiments:

- (1) Two-dimensional distortions of the return stroke channel from a circular cross section,
- (2) Two-dimensional asymmetries from return stroke displacement off the axis of the leader stroke, and
- (3) Three-dimensional distortions in the return stroke, such as the curvature of the channel axis shown in Fig. 1.

If we define a cylindrical coordinate system with the  $z$ -axis along the average direction of the channel axis (for channel sections which do not undergo large changes in direction), we find that all three types of asymmetry will produce a nonzero value of  $\xi_z$ . This will cause mixing in the  $(r,\theta)$  plane. In addition, for three-dimensional asymmetries,  $\xi_\theta$  will be non-negligible, producing mixing in the  $(r,z)$  plane (a vortex sheet). Fig. 2 shows that, for sufficiently short channel sections, all three types of asymmetry may be represented by a displacement  $\tilde{x}_0$  in the  $(r,z)$  plane, which causes the rotational symmetry about the  $z$ -axis to be broken. In our derivations, we will define the  $x$ -axis to be parallel to

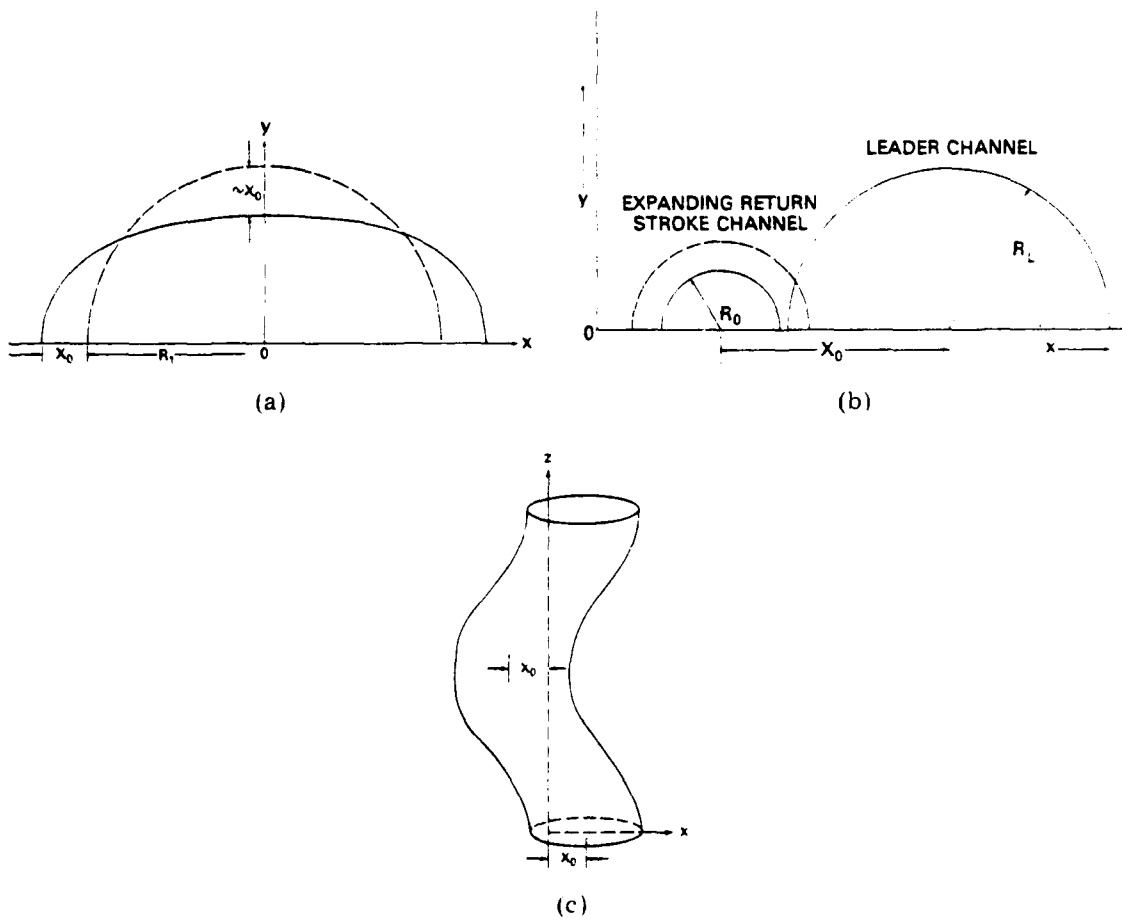


Fig. 2 — Schematic diagrams of three types of return stroke asymmetry which generate vorticity: (a) two-dimensional distortions (e.g., elliptical channel), (b) displacement from axis of leader channel, (c) three-dimensional distortions. The degree of asymmetry may be expressed in terms of the quantity  $X_0$  as indicated. In Fig. 2a and 2b, we show only the portion above the  $x - z$  symmetry plane.

$\tilde{x}_0$ . With this convention, Fig. 3 shows the flow field in the x-y plane for cases b and c in Fig. 2 after the return stroke channel has reached pressure equilibrium with the ambient air. This flow pattern is approximately equivalent to that of a vortex filament pair having average strengths of  $\pm \bar{\kappa}_z$  and located respectively at  $(\bar{x}, \pm \bar{y})$ . (The flow pattern for the elliptical channel in Fig. 2b is equivalent to the superposition of two vortex filament pairs. For simplicity we will discuss only a single vortex filament pair.) The average strength  $\bar{\kappa}_z$  is given by (Batchelor, 1967)

$$\bar{\kappa}_z(\tau) = \int_0^\infty dy \int_{-\infty}^\infty dx \zeta_z(x, y, \tau) \quad (3)$$

and the coordinates are

$$\bar{x}(\tau) = \frac{1}{\bar{\kappa}_z(\tau)} \int_0^\infty dy \int_{-\infty}^\infty dx x \zeta_z(x, y, \tau) \quad (4)$$

and

$$\bar{y}(\tau) = \frac{1}{\bar{\kappa}_z(\tau)} \int_0^\infty dy \int_{-\infty}^\infty dx y \zeta_z(x, y, \tau) \quad (5)$$

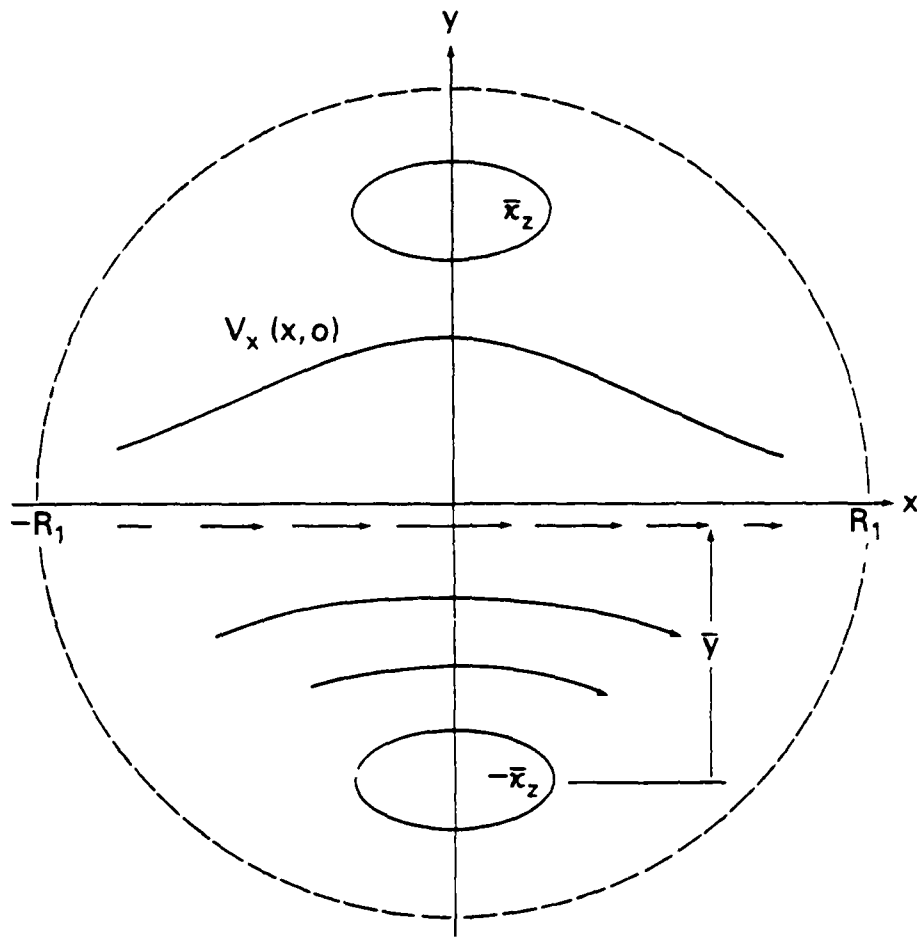
We obtain  $\zeta_z(x, y, \tau)$  by integrating (1) over the time interval  $(0, \tau)$ , where  $t = 0$  is the time of discharge initiation.

The vortex filament pair will migrate as a unit at a speed of

$$v_{\text{pair}} = \bar{\kappa}_z / 4\pi\bar{y} \quad (6)$$

in a direction parallel to the x-axis. The fluid velocity along the x-axis is

$$v_x(x, 0) = \bar{\kappa}_z \bar{y} / \pi (x^2 + \bar{y}^2) \quad (7)$$



$$\tau_{\text{mix}} = \frac{2\pi R_1}{|\bar{\kappa}_z| \bar{y}} [R_1^2/3 + \bar{y}^2]$$

Fig. 3 — Symmetric distribution of localized vorticity appears as two extended vortex filaments  $\bar{\kappa}_z$  separated by a distance  $2\bar{y}$ . Flow velocity induced by these vortices is shown along the  $x$  axis half-way between the filaments. The mixing time  $\tau_{\text{mix}}$  is defined here as the time it takes a fluid element at  $-R_1$  to reach  $R_1$  and hence effectively bisect the hot channel.

If we define a characteristic mixing time scale  $\tau_{\text{mix}}$  to be the time interval over which a fluid element travels along the x-axis from one "edge" of the channel to the opposite "edge," we may use (7) to obtain

$$\tau_{\text{mix}} = 2\pi R_1 (R_1^2/3 + \bar{y}^2) / |\bar{\kappa}_z| \bar{y} \quad (8)$$

where  $R_1$  is the approximate radius of the return stroke channel when pressure equilibrium is reached. We may, therefore, characterize the mixing time scale if we know the vorticity strength and the average displacements of the equivalent vortex pair from the (x,z) symmetry plane.

We have performed the integral in (3) by using (1) in conjunction with the following assumptions:

(1) We treat the return stroke as an instantaneous pressure pulse of finite size with a given radial profile and with a total energy deposition equivalent to that of a return stroke. The assumption of instantaneous deposition fits closely the experimental situation of Fig. 1. At the same time, we do not parallel the work of Hill, (1971, 1979), who permits energy to be deposited over a time interval  $\sim 100 \mu\text{s}$ . However, the formalism which we have developed is adequate for this latter case as well.

(2) The time  $\tau$  in (3) is equal to the time required for the return stroke channel to achieve pressure equilibrium with the surrounding atmosphere. For times  $t > \tau$  a residual vorticity exists, and this vorticity is responsible for convective cooling of the lightning channel.

(3) During expansion of the return stroke channel, the fluid outside the expanding region behaves incompressibly and the interior region expands uniformly. Thus the radial dependence of the fluid velocity is given by

$$v_r(r, t) = \begin{cases} \frac{U(t) r}{R(t)} & r \leq R(t) \\ \frac{U(t) R(t)}{r} & r > R(t) \end{cases} \quad (9)$$

where the boundary of the heated region is  $R(t)$  and the velocity of the boundary is  $U(t) = \dot{R}(t)$ . This assumption appears to be reasonable since the shock wave carries away only about 10% of the total energy deposited by the return stroke. Further, this assumption is more accurate when the energy deposition is slower. Notice that the acceleration is radial and has values strictly appropriate only if the effects of the nonaligned density gradients on the driving expansion flow are small.

(4) We approximate the integrand in (3) in terms of its value at time  $t=t_m$ , at which the expansion flux  $R_m U_m \equiv R(t_m) U(t_m)$  is a maximum. Under the above conditions, we obtain for the residual vorticity

$$\bar{\omega}_z(t) \approx \bar{\omega}_z(\tau) \approx U_m (R_1 - R_0) \bar{\rho}_n (c_\infty/c_0) f(R_0, R_1, R_m, X_0) \quad (10)$$

for the average z-component of the vorticity strength where  $t \geq \tau$ . The quantities  $R_0$  and  $R_1$  are, respectively, the initial average radius of the heated (return stroke) region and the average radius following expansion, and  $\rho_\infty$  is the ambient density. The quantity  $\rho_0$  is the density at the center of the return stroke channel for asymmetry types 1 and 3 (two and three dimensional distortions of the return stroke channel). For asymmetry type 2 (return stroke displacement off the leader channel axis),  $\rho_0$  is the density at the center

of the leader channel. The dimensionless form factor  $f$  is a complicated integral which contains geometric effects, detailed hydrodynamical interactions and information about the leader and return stroke pressure and density profiles. For asymmetry type 2, we have evaluated the form factor,  $f_2$ , for several different pressure and density profiles and have found that  $f_2$  is not strongly profile dependent. The values of  $|f_2|$  vary smoothly from zero at  $X_0/R_1 = 0$  to a peak of  $\leq 0.5$  at  $X_0/R_1 \sim 1$ . The values then decrease somewhat more slowly to zero as  $X_0/R_1$  increases beyond a value of  $\sim 1$ . Similar behavior occurs for the other asymmetry types. For rough estimates of  $|f_2|$ , a value of  $|f_2| \sim \frac{1}{3}$  is permissible, and we may substitute  $c_s$  for  $U_m$ , where  $c_s$  is the speed of sound at the axis of the return stroke when the current flow begins ( $t = 0$ ).

We have performed preliminary detailed simulations of the problem using the FAST2D computer code (Boris, 1977) to validate and calibrate the approximate analytic model developed above. In addition to accounting for shocks properly, which the theoretical model does not do, the simulations are capable of describing the late-time motions and profiles as modified by the induced vorticity. As above, we have treated the return stroke as an instantaneous pulse of finite size and equivalent energy rather than depositing the energy over a characteristic time interval ( $\sim 100 \mu s$ ). These simulations have indicated that the above analytic model and the resulting formula given in (10) will, in most cases, provide estimates of  $\bar{n}_2$  which differ from the simulation results by less than 30%. We have discovered that only modest asymmetry ( $X_0 \sim R_1/10$ ) is required to generate considerable mixing and that for a wide range of values of  $X_0/R_1$  ( $0.1 \leq X_0/R_1 \leq 1.5$ ) the residual vorticity and mixing rate vary by less than 30%.

Preliminary investigations of the asymmetries of type (3), i.e., three-dimensional distortions of the return stroke profile, indicate that (10) holds for  $\bar{\lambda}_e$  as well. For cases in which more than one type of asymmetry are present, the cumulative effects should increase the mixing rate, and the channel should cool more quickly. This would explain the faster cooling rates for electric discharges guided by preformed laser channels, since some displacement of the discharge axis from the axis of the preformed laser channel would be expected as well as three-dimensional distortion of the electric discharge channel.

We can now analyze the mixing shown in Fig. 1, which we assume in this case to be due primarily to three-dimensional curvature with a value of  $X_0/R_1 \sim 0.25$ . We have  $R_0 \sim 0.1$  cm (measured from open shutter photographs of the discharges),  $R_1 \sim 1.4$  cm,  $\rho_\infty/\rho_0 \sim 10$ ,  $|f_3| \sim \frac{1}{3}$  and  $U_m \sim c_s \sim 3.5 \times 10^4$  cm/s. From (10) we calculate  $\bar{\lambda}_z \sim 3.5 \times 10^4$  cm<sup>2</sup>/s. Using (8), and  $\bar{y} \sim 0.8 R_1$  (from our simulations), we obtain  $\tau_{mix} \approx 430$   $\mu$ s. From Fig. 1, we notice that violent perturbations begin to occur sometime between  $\sim 250 \mu$ s and  $\sim 900 \mu$ s. This is consistent with the definition and value of  $\tau_{mix}$ .

From Fig. 1, we also find that, for the laboratory experiments, reasonably complete mixing occurs at a time  $\Delta t_{cool} \sim 10^4$   $\mu$ s, which is  $\sim 20\tau_{mix}$  following discharge initiation. Referring to our discussion of the laboratory discharges in Fig. 1, we see that the volume increase of the channel  $\Delta V_{cool}$  (during the interval  $\Delta t_{cool}$ ) is also  $\sim 20 V_0$ , where  $V_0$  is the initial volume. We have found that, in general for convective cooling, (Appendix A),

$$\frac{\Delta t_{cool}}{\tau_{mix}} \approx \frac{\Delta V_{cool}}{V_0} . \quad (11)$$

The ratio on the right hand side of (11) depends only on the temperature of the channel before appreciable mixing occurs and the ambient temperature. For our laboratory discharges and lightning, these temperatures are approximately

the same. Thus, we assume that for lightning  $t_{\text{cool}} \sim 20 \tau_{\text{mix}}$ , from which we may obtain rough estimates of the time required for "complete" cooling of a return stroke channel and of the average mixing rate. For lightning we assume (Hill et al., 1980)  $R_0 \sim 1\text{cm}$ ,  $R_1 \sim 16\text{cm}$ ,  $r_{\infty}/r_0 \sim 10$ ,  $f_1 \sim \frac{1}{3}$ , and  $U_m \sim c_s \sim 5 \times 10^4 \text{cm/s}$ . From (10) we obtain  $\bar{v}_2 \sim 56 \times 10^4 \text{cm}^2/\text{s}$ . Using (8) with  $\bar{y} \sim 0.8 R_1$ , we find  $\tau_{\text{mix}} \sim 3.4 \times 10^{-3} \text{s}$ . Thus we expect "complete mixing" to occur in  $\sim 68 \times 10^{-3} \text{s}$  after energy deposition by the return stroke. If, as in Fig. 1, the volume of the channel increases to  $\sim 20$  times its original value during that time, we will have  $\sim 20 \text{cm}^3$  of ambient air mixed with each  $1 \text{cm}^3$  of air initially in the channel. This gives us a mixing rate ( $F_0$  in the notation of Hill et al., 1980) of  $\sim 300 \text{cm}^3/\text{s}$  per  $\text{cm}^3$  of air originally in the channel, which falls in the upper end of the range considered by Hill et al. Because we have not treated the cumulative effects of the various asymmetry types and because some of the numbers which we have used are only rough estimates, we feel that  $300 \text{cm}^3/\text{s}$  should be treated as an order of magnitude estimate of  $F_0$ . Given our results, the estimates of Hill et al. (1980) for global  $\text{NO}_x$  production by lightning appear to be quite reasonable.

### Acknowledgments

This paper reports the results of work which was performed at the Naval Research Laboratory by members of the Laboratory for Computational Physics and the Plasma Physics Division. The Office of Naval Research and the Defense Advanced Research Projects Agency provided the funding for this work. The authors also gratefully acknowledge the helpful comments of Dr. A. E. Robson during the preparation of this report.

## References

Batchelor, G. K., 1967: An Introduction to Fluid Dynamics, New York, Cambridge University Press, 507 - 593.

Boris, J. P., 1977: Dynamic Stabilization of the Imploding Shell Rayleigh-Taylor Instability, Comments on Plasma Physics and Controlled Fusion (3), No. 1, 1-13.

Greig, J. R., D. W. Koopman, R. F. Fernsler, R. E. Pechacek, I. M. Vitkovitsky, and A. W. Ali, 1978: Electrical Discharges Guided by Pulsed CO<sub>2</sub> - Laser Radiation, Phys. Rev. Lett., 41, 174-177.

Hill, R. D., 1971: Channel Heating in Return-Stroke Lightning, J. Geophys. Res., 76, 637 - 645.

Hill, R. D., 1979: On the Production of Nitric Oxide by Lightning, Geophys. Res. Lett., 6, 945 - 947.

Hill, R. D., R. G. Rinker, and H. Dale Wilson, 1980: Atmospheric Nitrogen Fixation by Lightning, J. Atmos. Sci., 37, 179 - 192.

#### Footnotes

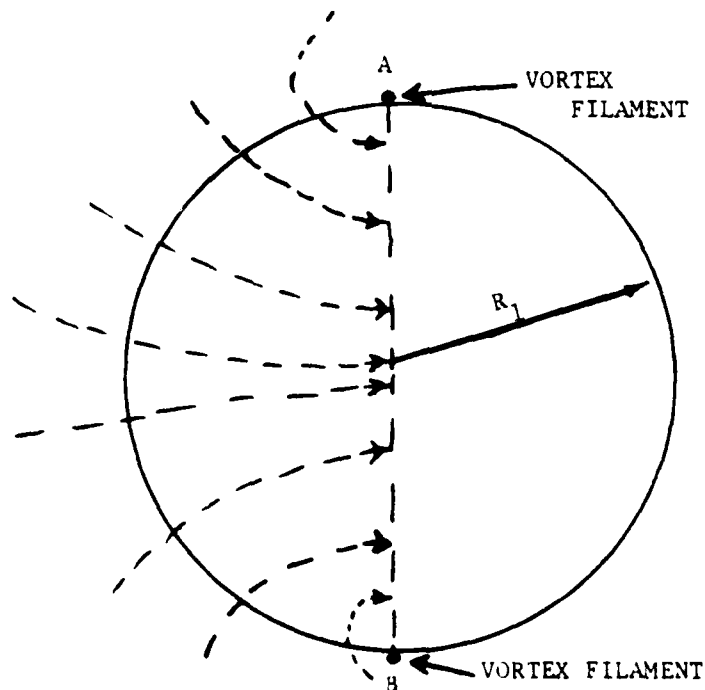
1. JAYCOR, Inc., Alexandria, Virginia
2. Boris, J. P., and J. M. Picone, 1980; "Beam Generated Vorticity and Convective Channel Mixing," NRL Memorandum Report 4327, [available through DDC and NTIS].

APPENDIX A

In this appendix, we give a heuristic proof of the relation (11) for convective cooling of discharge channels:

$$\frac{\Delta V_{\text{cool}}}{V_0} \approx \frac{\Delta t_{\text{cool}}}{\tau_{\text{mix}}} . \quad (11)$$

We define  $\Delta t_{\text{cool}}$  to be the time interval during which the channel cools convectively to ambient temperature;  $\Delta V_{\text{cool}}$  is the increase in channel volume due to entrainment of ambient air over the time interval  $\Delta t_{\text{cool}}$ ;  $V_0$  is the channel volume before appreciable mixing; and  $\tau_{\text{mix}}$  has been defined as the time required for a fluid element to move from one side of the channel to the opposite side. We assume that the channel is cylindrical with radius  $R_1$  and length  $Z$  and that a vortex filament pair exists at  $\bar{x} = 0, \bar{y} \approx \pm R_1$ .



Fluid elements on different streamlines move at different speeds, and thus adjacent fluid elements on different streamlines will soon have different temperatures and densities. Thermal conduction and molecular diffusion will occur rapidly between adjacent fluid elements since their displacement is small, and we therefore have enhanced cooling over the same situation (hot channel in cool ambient air) without convection. In addition, the experimental data (see Fig. 1) indicate that turbulent mixing occurs as the surrounding air is pulled into the hot channel. These factors should combine to produce rapid, efficient mixing, and the continued entrainment of ambient air will cause the channel to expand. To obtain the volume increase over the interval  $\Delta t_{\text{cool}}$ , we may therefore compute the volume of ambient air flowing into the channel per unit time. This is given by (Batchelor, pp. 75-76)

$$\frac{dV}{dt} = \int_{\substack{\text{SURFACE} \\ \text{ABZ}}} \underline{v} \cdot \underline{da} \quad (1A)$$

where  $\underline{v}$  is the fluid velocity and the integral is taken over the surface defined by the channel axis Z and the dashed line  $\overline{AB}$  in the figure. Given the definition of  $\tau_{\text{mix}}$ , we may approximate v by:

$$v \sim \frac{2R_1}{\tau_{\text{mix}}} \quad (2A)$$

The area of the surface  $\overline{ABZ}$  is

$$a = 2R_1 Z. \quad (3A)$$

Thus the volume of ambient air flowing into the channel per unit time is

$$\frac{dV}{dt} \sim \frac{2R_1}{\tau_{mix}} \times 2R_1 Z = \frac{4R_1^2 Z}{\tau_{mix}} \quad (4A)$$

We now estimate the volume increase of the channel ( $\Delta V_{cool}$ ) during the cooling time interval ( $\Delta t_{cool}$ ) by integrating (4A) over  $\Delta t_{cool}$ . This gives us

$$\Delta V_{cool} \sim \frac{dV}{dt} \Delta t_{cool} \sim \frac{4R_1^2 Z}{\tau_{mix}} \Delta t_{cool} \quad (5A)$$

The original channel volume is given by

$$V_0 = \pi R_1^2 Z \quad (6A)$$

so that

$$\frac{\Delta V_{cool}}{V_0} \sim \frac{4}{\pi} \frac{\Delta t_{cool}}{\tau_{mix}} \sim \frac{\Delta t_{cool}}{\tau_{mix}} \quad (7A)$$

This relation is independent of initial channel size, and the volume increase will be primarily determined by the channel temperature  $T_1$  just before mixing begins and the ambient temperature  $T_\infty$ . For both lightning and the laboratory discharges  $T_1 \sim 3000-5000$  K and  $T_\infty \sim 300$  K. Thus

$\frac{\Delta V_{cool}}{V_0}$  and  $\frac{\Delta t_{cool}}{\tau_{mix}}$  are about the same in the two cases. So our use of

$\Delta t_{cool} \sim 20 \tau_{mix}$  for lightning appears to be justified.

We note that (1A) can be restated as

$$\frac{\Delta V_{cool}}{\Delta t_{cool}} = \frac{V_0}{\tau_{mix}} \quad (8A)$$

The left hand side is just the average "mixing rate" for the problem. Thus the factor  $\tau_{\text{mix}}$  indeed appears to be a fundamental time scale for convective channel cooling. Further investigation of the physical significance of  $\tau_{\text{mix}}$  should result in a more elegant proof of (11).

DISTRIBUTION LIST

1. Commander  
Naval Sea Systems Command  
Department of the Navy  
Washington, D.C. 20363  
ATTN: NAVSEA 03H (Dr. C. F. Sharn)
2. Central Intelligence Agency  
P. O. Box 1925  
Washington, D. C. 20013  
ATTN: Dr. C. Miller/OSI
3. Air Force Weapons Laboratory  
Kirtland Air Force Base  
Albuquerque, New Mexico 87117  
ATTN: Lt. Col. J. H. Havey  
Maj. Harold Dogliani  
Dr. David Straw
4. U. S. Army Ballistics Research Laboratory  
Aberdeen Proving Ground, Maryland 21005  
ATTN: Dr. D. Eccleshall (DRXBR-BM)
5. Ballistic Missile Defense Advanced Technology Center  
P. O. Box 1500  
Huntsville, Alabama 35807  
ATTN: Dr. L. Harvard (BMDSATC-1)
6. B-K Dynamics Inc.  
15825 Shady Grove Road  
Rockville, Maryland 20850  
ATTN: Mr. I. Kuhn
7. Intelcom Rad Tech  
P. O. Box 81087  
San Diego, California 92183  
ATTN: Mr. W. Selph
8. Lawrence Livermore Laboratory  
University of California  
Livermore, California 94550  
ATTN: Dr. R. J. Briggs  
Dr. T. Fessenden  
Dr. E. P. Lee
9. Mission Research Corporation  
735 State Street  
Santa Barbara, California 93102  
ATTN: Dr. C. Longmire  
Dr. N. Carron

10. Pulse Sciences Inc.  
Suite 610  
1615 Broadway  
Oakland, California 94612  
ATTN: Dr. S. Putnam
11. Science Applications, Inc.  
1200 Prospect Street  
LaJolla, California 92037  
ATTN: Dr. M. P. Fricke  
Dr. W. A. Woolson
12. Science Applications, Inc.  
Security Office  
5 Palo Alto Square, Suite 200  
Palo Alto, California 94304  
ATTN: Dr. R. R. Johnson  
Dr. Leon Feinstein  
Dr. J. G. Siambis
13. Science Applications, Inc.  
1651 Old Meadow Road  
McLean, Virginia 22101  
ATTN: Mr. W. Chadsey
14. Science Applications, Inc.  
8201 Capwell Drive  
Oakland, California 94621  
ATTN: Dr. J. E. Reaugh
15. Naval Surface Weapons Center  
White Oak Laboratory  
Silver Spring, Maryland 20910  
ATTN: Mr. R. J. Biegalski  
Dr. R. Cawley  
Dr. J. W. Forbes  
Dr. D. L. Love  
Dr. C. M. Huddleston  
Mr. W. M. Hinckley  
Dr. G. E. Hudson  
Mr. G. J. Peters  
Mr. N. E. Scofield  
Dr. E. C. Whitman  
Dr. M. H. Cha  
Dr. H. S. Uhm  
Dr. R. B. Fiorito
16. C. S. Draper Laboratories  
Cambridge, Massachusetts 02139  
ATTN: Dr. E. Olsson  
Dr. L. Matson

17. M. I. T. Lincoln Laboratories  
P. O. Box 73  
Lexington, Massachusetts 02173  
ATTN: Dr. J. Salah
18. Physical Dynamics, Inc.  
P. O. Box 1883  
LaJolla, California 92038  
ATTN: Dr. K. Brueckner
19. Office of Naval Research  
Department of the Navy  
Arlington, Virginia 22217  
ATTN: Dr. W. J. Condell (Code 421)
20. Avco Everett Research Laboratory  
2385 Revere Beach Pkwy.  
Everett, Massachusetts 02149  
ATTN: Dr. R. Patrick  
Dr. Dennis Reilly
21. Defense Technical Information Center  
Cameron Station  
5010 Duke Street  
Alexandria, Virginia 22314 (12 copies)
22. Naval Research Laboratory  
Washington, D. C. 20375  
ATTN: M. Lampe - Code 4792  
M. Friedman - Code 4700.1  
J. R. Greig - Code 4763 (50 copies)  
I. M. Vitkovitsky - Code 4770  
T. Coffey - Code 4000  
Superintendent, Plasma Physics Div. - Code 4700 (25 copies)  
Library - Code 2628 (20 copies)  
A. Ali - Code 4700.1T  
D. Book - Code 4040  
J. Boris - Code 4040  
S. Kainer - Code 4790  
A. Robson - Code 4760  
M. Picone - Code 4040  
D. Spicer - Code 4169  
M. Raleigh - Code 4763  
R. Pechacek - Code 4763  
J. D. Sethian - Code 4762  
K. A. Gerber - Code 4762  
D. N. Spector - Code 4762
23. Defense Advanced Research Projects Agency  
1400 Wilson Blvd.  
Arlington, Virginia 22209  
ATTN: Dr. J. Mangano  
Dr. J. Bayless

24. JAYCOR  
205 S. Whiting St.  
Alexandria, Virginia 22304  
ATTN: Drs. D. Tidman  
R. Hubbard  
J. Gillory
25. JAYCOR  
Naval Research Laboratory  
Washington, D. C. 20375  
ATTN: Dr. R. Fernsler - Code 4770  
Dr. G. Joyce - Code 4790  
Dr. S. Goldstein - Code 4770
26. SAI  
Naval Research Laboratory  
Washington, D. C. 20375  
ATTN: A. Drobot - Code 4790  
W. Sharp - Code 4790
27. Physics International, Inc.  
2700 Merced Street  
San Leandro, California 94577  
ATTN: Dr. J. Maenchen  
Dr. E. Goldman
28. Mission Research Corp  
1400 San Mateo, S.E., Suite A  
Albuquerque, New Mexico 87108  
ATTN: Dr. Brendan Godfrey  
Dr. Carl Ekdahl
29. Princeton University  
Plasma Physics Laboratory  
Princeton, New Jersey 08540  
ATTN: Dr. F. Perkins, Jr.
30. McDonnell Douglas Research Laboratories  
Dept. 223, Bldg. 33, Level 45  
Box 516  
St. Louis, Missouri 63166  
ATTN: Dr. Michael Greenspan  
Dr. J. C. Leader
31. Cornell University  
Ithaca, New York 14853  
ATTN: Prof. David Hammer
32. Sandia Laboratories  
Albuquerque, New Mexico 87185  
ATTN: Dr. Bruce Miller  
Dr. Barbara Epstein  
Dr. John Olsen  
Dr. Don Cook

33. University of California  
Physics Department  
Irvine, California 92717  
ATTN: Dr. Gregory Benford
34. Naval Air Systems Command  
Washington, D. C. 20361  
ATTN: Dr. R. J. Wasneski, Code AIR-350F
35. Beers Associates, Inc.  
P. O. Box 2549  
Reston, Virginia 22090  
ATTN: Dr. Douglas Strickland
36. U. S. Department of Energy  
Washington, D. C. 20545  
Office of Fusion Energy, ATTN: Dr. W. F. Dove  
Office of Inertial Fusion, ATTN: Dr. T. Godlove
37. AFOSR/NP  
Bolling Air Force Base  
Washington, D. C. 20331  
ATTN: Capt. R. L. Gullickson